

Generalized Tube Model of Biased Reptation for Gel Electrophoresis of DNA

JAAN NOOLANDI, GARY W. SLATER, HWA AUN LIM,
JEAN LOUIS VIOVY

A theoretical analysis of the reptational motion of DNA in a gel that includes the effects of molecular fluctuations has been used to explain the main features found in experiments involving periodic inversion of the electric field. The resonance-like decrease of the electrophoretic mobility as a function of pulse duration is related to transient "undershoots" in the orientation of the molecule, in agreement with recent experimental data. These features arise from a delicate interplay of internal and center of mass motion of the molecules under pulsed field conditions, and are important for the separation of DNA molecules in the size range 0.2 to 10 million base pairs.

IN THE LAST FEW YEARS AN INTENSIVE effort has been ongoing, both experimentally (1-6) and theoretically (7-12), to study the molecular motion underlying the optimum separation conditions for gel electrophoresis. The first theories were based on tube models (7-10), where the average molecular conformation was approximated by a primitive chain of rigid segments moving in a narrow tube; these models were ideally suited for exploiting recent advances made in the dynamics of polymer melts (13). The tube model was successful in predicting the phenomenon of band inversion, which arises from the occasional trapping of large DNA molecules in slow-moving, U-shaped conformations and which leads to the breakdown of the rule that the smallest fragments always have the largest mobilities (10). On the whole, the original tube models worked well when local, intratube molecular motion could be neglected.

The more advanced separation techniques, such as field-inversion gel electrophoresis (FIGE), have shown that the internal modes of the molecule play a key role in the molecular mechanism responsible for the separation (2, 4, 11, 12). The rigid tube model cannot explain the resonance-like decrease in electrophoretic mobility as a function of pulse duration found in FIGE techniques, since the predicted molecular conformations are essentially symmetrical with respect to field inversion.

J. Noolandi and G. W. Slater, Xerox Research Center of Canada, 2660 Speakman Drive, Mississauga, Ontario, Canada L5K 2L1.

H. A. Lim, Supercomputer Computations Research Institute, Florida State University, Tallahassee, FL 32306.

J. L. Viovy, Laboratoire de Physico-Chimie Théorique, ESPCI, 10 rue Vauquelin, 75231 Paris Cedex 05, France.

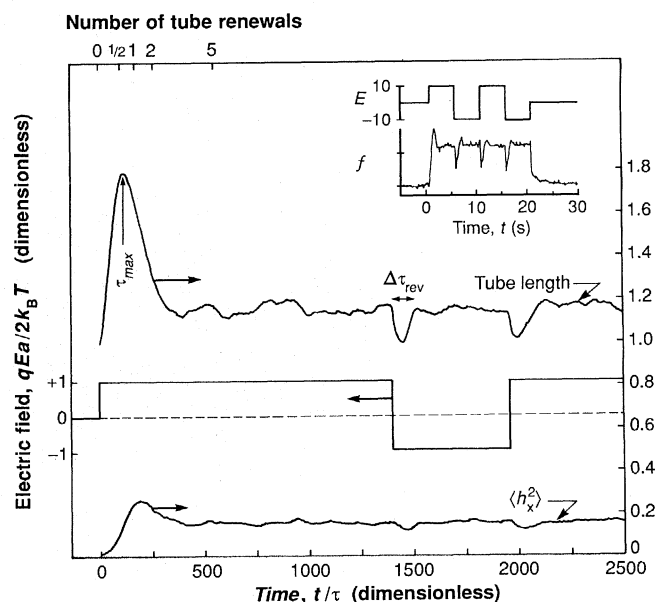
We propose a generalization of the tube model, in which the DNA molecule is represented by a set of connected, flexible entropic springs (Rouse chain) that follows the axis of a tube and that evolves according to the principles of the reptation model (8-10). The basic characteristics of the model are as follows: Let $s(i, t)$ be the position of the i th bead at time t along the tube axis. For simplicity, the N beads are initially placed in the middle of N consecutive pores of size a , with a the average length of each of the $N - 1$ springs in the absence of a field. The initial tube conformation is assumed to be a random walk in three-dimensional space. The equation of motion for the position of a

bead (with a charge q) along the tube axis is given by

$$\xi \frac{\partial s(i, t)}{\partial t} = F_s(i, i+1) - F_s(i, i-1) + qE \cos\theta(i, t) + \eta(i, t)$$

where ξ is the friction coefficient of one bead, $F_s(i, i+1)$ [$= F_s(|s(i, t) - s(i+1, t)| \geq 0)$] is the entropic (spring) force between two beads [given by the inverse Langevin function (14)], q is the charge on each of the beads, $\theta(i, t)$ is the angle between the local tube axis and the field direction (chosen as x here), E is the magnitude of the electric field, and $\eta(i, t)$ is the random force acting on bead i , with $\langle \eta(i, t) \eta(j, t') \rangle = 2\xi k_B T \delta_{ij} \delta(t - t')$, where k_B is the Boltzmann constant, T is the absolute temperature, and δ_{ij} and $\delta(t - t')$ are the Kronecker and Dirac delta functions, respectively. As in any tube model, an entropic force proportional to $k_B T$ is exerted on each of the two end beads, which prevents the chain from collapsing inside its tube (13); this entropic force is due to the two end beads moving in a three-dimensional space and thus having more degrees of freedom than those beads trapped inside the tube. The evolution of the two end beads follows the normal rules of reptational motion (13), that is, new tube sections are created in random directions when the first or the N th bead leaves the tube. Hence, the tube guides the overall motion of the DNA molecule, which in turn is allowed to fluctuate longitudinally inside the tube. The only mode of motion that is not described by this model is the development and relaxation of transverse modes

Fig. 1. Relative average tube length $\langle s(N, t) - s(1, t) \rangle / Na$ (upper curve) and end-to-end distance $\langle h_x^2 \rangle / N^2 a^2 = \langle [x(N, t) - x(1, t)]^2 \rangle / N^2 a^2$ (lower curve) of an $N = 30$ bead chain as a function of time (in units of $\tau = \xi a^2 / 2k_B T$) when an electric field is applied to an initial random-walk tube configuration. The scaled electric field $qEa/2k_B T$ is given by the middle line. The upper x -axis gives the curvilinear position $\langle s(N/2, t) \rangle / Na$ of the center bead of the chain, a measure of the number of tube renewals undergone by the chain. The average was made from 500 chains with different initial configurations, and the field was reversed at times $t = 1400\tau$ and $t = 1960\tau$. The maximum spring length was $l = 4a$ in this simulation. The inset shows the orientation of a DNA during a short field inversion sequence from Holzwarth *et al.* [adapted from figure 7 of (6)]; f is the orientation function measured by fluorescence-detected linear dichroism (6) and E is the electric field (volts per centimeter).



such as “hernias,” in which local fluctuations of the molecule result in some amount of material venturing outside the average tube surface for an extended period of time.

We now present some numerical results obtained by using this model to carry out computer simulations. When the electric field is first applied, the average tube length $\langle s(N,t) - s(1,t) \rangle$ increases suddenly, reaches a maximum at time $t = \tau_{\max}$, and then decreases to a steady-state value (Fig. 1). This overstretching of the molecule occurs because both ends initially move in the field direction in response to the electric forces; this process stops when the elastic forces, which increase when the entropic springs stretch, become large enough to dominate the electric forces. The recoil that follows reduces the tube length rapidly until the steady-state value is reached, and one end of the chain becomes the sole head of the reptative motion. The square of the end-to-end distance of the chain in the field direction, $\langle (h_x^2) \equiv \langle [x(N,t) - x(1,t)]^2 \rangle$, also increases in the presence of a field. Both $\langle s(N,t) - s(1,t) \rangle$ and $\langle [x(N,t) - x(1,t)]^2 \rangle$ obtain steady-state values that are larger in the presence of the field; note that the average orientation of a tube segment, $\langle [x(N,t) - x(1,t)]^2 \rangle^{1/2} / \langle s(N,t) - s(1,t) \rangle$, is of order $qEa/6k_B T$, as predicted by analytical calculations (9). When the field is reversed, the tube length goes through a minimum (having a width in time of $\Delta\tau_{\text{rev}}$) before it regains its steady-state value. During this transient regime, the velocity $V_x(t)$ of the center-of-mass of the molecule is larger than in the steady-state regime. Results for molecular sizes $N = 15, 30, 45$, and 60 and a field $qEa/2k_B T = 1.0$ indicate that both τ_{\max} and $\Delta\tau_{\text{rev}}$ scale like N^k , with $1 < k \leq 3/2$; preliminary results also indicate that $\tau_{\max} \propto E^{-m}$, with $1/2 \leq m \leq 1$.

An initial overshoot and a decrease in tube orientation when the field is reversed have been observed by Holzwarth *et al.* (6) using fluorescence-detected linear-dichroism (see insert of Fig. 1). They also observed (15) that the chain had moved over a distance approximately equal to half its contour length at time $t = \tau_{\max}$, in agreement with the upper x -axis on Fig. 1, which shows that the relative curvilinear position $\langle |s(N/2,t)| \rangle / Na$ of the center bead of the chain, a measure of the number of tube renewals undergone by the chain, is of order 0.5 for $t = \tau_{\max}$. Their results also indicate that $\tau_{\max} \propto NE^{-1}$, in fair agreement with our findings.

The electrophoretic velocity varies with pulse duration t_p in a FIGE configuration, as shown in Fig. 2. A gradual increase of the velocity occurs when the pulse duration t_p is increased from $t_p \ll \tau_{\text{dis}}/N$ to $t_p \gg \tau_{\text{dis}}$,

where τ_{dis} is the tube disengagement (or renewal) time at steady state; this is in agreement with the argument of Viovy (12) concerning the effect of very high frequency fields in FIGE, and has been observed experimentally (16). However, the curve also shows a marked minimum for a critical pulse duration $t_p = \tau^* \approx \Delta\tau_{\text{rev}}$; since $\Delta\tau_{\text{rev}}$ is proportional to the molecular size, this sudden decrease of the velocity permits the separation of large molecules that cannot be separated in continuous fields. Our power law $\tau^* \approx \Delta\tau_{\text{rev}} \propto N^k$, with $1 < k \leq 3/2$, is in good agreement with FIGE results (16).

This resonance-like effect of the pulses on electrophoretic velocity is the effect observed by Carle *et al.* (2) under similar conditions, and by Lalande *et al.* with two different fields (4), and represents the basic phenomenon exploited by FIGE-like separation techniques.

The mechanisms involved in the decrease of the tube length that occurs upon field reversal are apparently responsible for the increased power of separation of FIGE. In order to understand these mechanisms, we studied the intratube distribution of DNA during migration. The average spring length $\langle |s(i+1,t) - s(i,t)| \rangle / a$ as a function of the spring index $i/(N-1)$, $[1 \leq i \leq N-1]$, is shown in Fig. 3. Since the average tube length is larger than in the absence of a field (see Fig. 1), most springs are slightly over-stretched; however, there is a net asymmetry in the distribution of the overstretching inside the tube, with the springs near the head of the reptating molecule being in fact compressed, the springs in the middle very over-stretched, and the tail springs only slightly over-stretched. Note also that this asymmetry is steeper for larger molecular sizes. When the field is reversed, this asymmetrical distribution has to be reversed before the steady state can be achieved; this process takes a time $\tau^* \approx \Delta\tau_{\text{rev}}$ and is responsible for the different velocity of the molecule just after the field is switched.

At least two mechanisms can participate in the buildup of this asymmetry. First, tube length fluctuations may cause the last bead (or tail bead) of the chain to leave the tube even though the field does not favor it; in this case, a J-shaped conformation is formed that can affect the velocity of the chain, if the field is reversed before the small arm of the J retracts inside the tube (12). In this type of conformation, the tail end of the tube tends to point and move in the field direction for a while, which stretches the tail end of the chain in much the same way as the overstretching for times $t \approx \tau_{\max}$. Second, when a new tube section is created with an orientation not favored by the field, the head bead probably does not reach the end of the

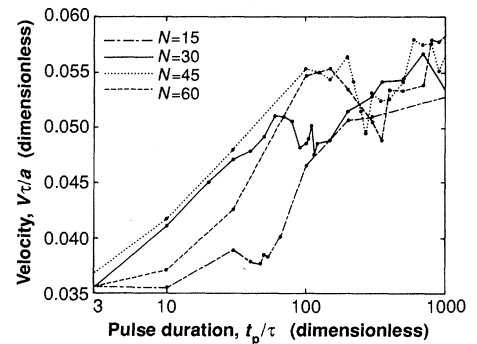


Fig. 2. Average center-of-mass velocity of a DNA molecule in field inversion electrophoresis as a function of the forward pulse duration t_p (in units of $\tau = \xi a^2/2k_B T$). The field intensity was $qEa/2k_B T = +1.0$ during the forward pulses of duration t_p , and $qEa/2k_B T = -1.0$ during the reverse pulses of duration $0.4t_p$ (the ratio between the two pulse durations is kept constant). The maximum spring length was chosen to be $l = 4a$ in this simulation, and the duration of the migration was $10^5\tau$.

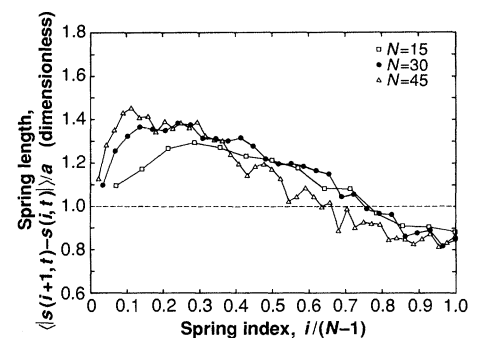


Fig. 3. Average spring length $\langle |s(i+1,t) - s(i,t)| \rangle / a$ as a function of the spring index $i/(N-1)$ under steady-state conditions in a constant electric field $qEa/2k_B T = +1.0$. The $(N-1)$ th spring is defined as the one pointing in the field direction (“the head”). The dashed line gives the average zero-field extension of the springs. The maximum spring length was chosen to be $l = 4a$ in this simulation, and the average was made over 400 chains (200 chains for 45 beads) at a given time $t \gg \tau_{\max}$.

pore; instead, it would return inside the tube and a new tube section would need to be created. These “hesitations” of the head bead, which are responsible for the average orientation of a tube section $\langle [x(N,t) - x(1,t)]^2 \rangle^{1/2} / \langle s(N,t) - s(1,t) \rangle$ being larger in the presence of a field, also mean that the rest of the chain tends to catch up with the motion of the head bead giving compressed springs near the front of the chain. These results are in qualitative agreement with the recent results of Deutsch (11) in which a two-dimensional computer simulation indicated that the DNA segments near the head of the reptating chain tend to bunch up, with an increased probability of having U-shaped conformations similar to those responsible for band inversion in continuous fields (10). Similar effects can be obtained in

our one-dimensional model as long as the chain is allowed to fluctuate inside its tube.

The model presented here has two major advantages: (i) it is simple enough to be amenable to analytical analysis, and (ii) the effect of the internal modes can be singled out and interpreted by comparing the results of this model with those of the original biased reptation model (10), which replaces the springs by rigid rods. However, only longitudinal fluctuations (those along the tube axis) are allowed in this model, which clearly reduces the total effect of the fluctuations available to the molecule in a gel. Transverse fluctuations, including hernias, are expected to play an important role in this system, especially in high fields and for long molecules. Nonhomogeneous gels may also increase the effect of the fluctuations. Hernias may be responsible for U- and W-shaped conformations that can affect the mobility of DNAs in FIGE. Taking into account these two types of conformations

would enhance the effect of the fluctuations and possibly increase the importance of the effects found upon field reversal; for example, the minima found on Fig. 2 would probably be deeper if more degrees of freedom would be allowed to the reptating fluctuating chains. The recent results of fluorescence-detected linear dichroism experiments can be interpreted in terms of intratube fluctuations (including both tube length fluctuations and nonhomogeneous spring stretching), and these fluctuations can explain the FIGE effect when the frequency of the pulsed field is in resonance with the relaxation time associated with the intratube fluctuations.

REFERENCES

1. D. C. Schwartz and C. R. Cantor, *Cell* **37**, 67 (1984).
2. G. F. Carl, M. Frank, M. V. Olson, *Science* **232**, 65 (1986).
3. P. Serwer, *Electrophoresis* **4**, 375 (1983); N. C.

- Stellwagen, *Biopolymers* **24**, 2243 (1985); M. Jonsson, B. Akerman, B. Norden, *ibid.* **27**, 381 (1988).
4. M. Lalande, J. Noolandi, C. Turmel, J. Rousseau, G. W. Slater, *Proc. Natl. Acad. Sci. U.S.A.* **84**, 8011 (1987).
5. E. M. Southern, R. Anand, W. R. A. Brown, D. S. Fletcher, *Nucleic Acids Res.* **15**, 5925 (1987); P. Serwer, *Electrophoresis* **8**, 301 (1987); B. W. Birren, E. Lai, S. M. Clark, L. Hood, M. I. Simon, *Nucleic Acids Res.* **16**, 7563 (1988).
6. G. Holzwarth, C. B. McKee, S. Steiger, G. Crater, *Nucleic Acids Res.* **15**, 10031 (1987).
7. L. S. Lerman and H. L. Frisch, *Biopolymers* **21**, 995 (1982).
8. O. J. Lumpkin, P. Déjardin, B. H. Zimm, *ibid.* **24**, 1575 (1985).
9. G. W. Slater and J. Noolandi, *ibid.* **25**, 431 (1986); K. Kremer, *Polym. Commun.* **29**, 292 (1988).
10. J. Noolandi, J. Rousseau, G. W. Slater, C. Turmel, M. Lalande, *Phys. Rev. Lett.* **58**, 2428 (1987).
11. J. M. Deutsch, *Science* **240**, 922 (1988).
12. J.-L. Viovy, *Phys. Rev. Lett.* **60**, 855 (1988).
13. M. Doi and S. F. Edwards, *The Theory of Polymer Dynamics* (Oxford Univ. Press, Oxford, 1986).
14. R. I. Tanner, *Engineering Rheology* (Oxford Univ. Press, Oxford, 1985).
15. G. Holzwarth, K. J. Platt, R. W. Whitcomb, C. B. McKee, *Biophys. J.* **53**, 407a (1988).
16. C. J. Bostock, *Nucleic Acids Res.* **16**, 4239 (1988).

17 November 1988; accepted 2 February 1989

Heat Flow and Hydrothermal Circulation in the Cascade Range, North-Central Oregon

S. E. INGEBRITSEN, D. R. SHERROD, R. H. MARINER

In north-central Oregon a large area of near-zero near-surface conductive heat flow occurs in young volcanic rocks of the Cascade Range. Recent advective heat flux measurements and a heat-budget analysis suggest that ground-water circulation sweeps sufficient heat out of areas where rocks younger than 6 Ma (million years ago) are exposed to account for the anomalously high advective and conductive heat discharge measured in older rocks at lower elevations. Earlier workers have proposed that an extensive midcrustal magmatic heat source is responsible for this anomalously high heat flow. Instead, high heat flow in the older rocks may be a relatively shallow phenomenon caused by regional ground-water flow. Any deeper anomaly may be relatively narrow, spatially variable, and essentially confined to the Quaternary (less than 2 Ma) arc. Magmatic intrusion at a rate of 9 to 33 cubic kilometers per kilometer of arc length per million years can account for the total heat flow anomaly. Deep drilling in the areas of high heat flow in the older rocks could indicate which model is more appropriate for the near-surface heat flow data.

QUATERNARY VOLCANOES OF THE Cascade Range form a 1200-km-long volcanic arc that extends from southern British Columbia to northern California. The arc is related to subduction of the Juan de Fuca Plate beneath North America. Detailed geologic mapping, measurements of advective heat discharge, and numerous conductive heat flow measurements are available for a 135-km-long section of the Cascade Range in north-central Oregon. This data set allows us to estimate fluxes of heat and mass (thermal fluid and magma) and to document the role of ground-water movement in redistributing heat in the up-

per crust. The results provide some insight into the thermal structure of the arc, and have implications for its geothermal resource potential.

In the study area (Fig. 1), the High Cascades physiographic subprovince is a broad constructional ridge of upper Pliocene and Quaternary (<3.3 Ma) volcanic rocks surmounted by several Quaternary stratovolcanoes. The High Cascades are flanked by Oligocene to lower Pliocene volcanic rocks of the Western Cascades to the west and Deschutes basin to the east. Western Cascades rocks also underlie the High Cascades; they are generally less permeable than the younger rocks. In this report, we use Western Cascades and High Cascades as

location terms. We also distinguish (i) the Quaternary (<2 Ma) arc, or area of Quaternary vents (Fig. 1), because older magmatic heat sources will generally have cooled to near ambient temperatures (1), and (ii) the region where uppermost Miocene (<6 Ma),

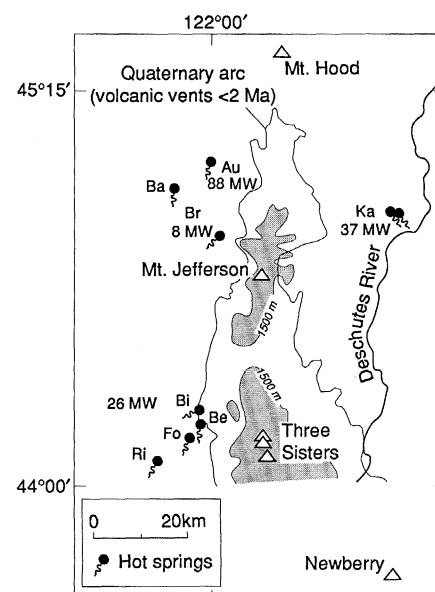


Fig. 1. Map showing the location of hot springs, the Quaternary arc, prominent volcanoes (Δ), the 1500-m-elevation contour, and the amount of heat transported advectively by the hot spring systems. The total for the southerly group of hot springs (~26 MW) is 1.5 times the value obtained from the individual spring groups (Table 1), because of diffuse input of thermal water into the surface drainage; hot springs: Au, Austin; Ba, Bagby; Br, Breitenbush; Bi, Bigelow; Be, Belknap; Fo, Foley; Ri, unnamed spring on Rider Creek; Ka, Kahneeta.